# Nonclassicality criteria for $N$-dimensional optical fields detected by quadratic detectors

Jan Peřina, Jr. [*] and Pavel Pavlíček

*Institute of Physics of the Czech Academy of Sciences,*
*Joint Laboratory of Optics of Palacký University and Institute of Physics of CAS,*
*17. listopadu 50a, 772 07 Olomouc, Czech Republic*

Václav Michálek, Radek Machulka, and Ondřej Haderka

*Joint Laboratory of Optics of Palacký University and Institute of Physics of the Czech Academy of Sciences,*
*Faculty of Science, Palacký University, 17. listopadu 12, 77146 Olomouc, Czech Republic*

Nonclassicality criteria for general $N$-dimensional optical fields are derived. They involve intensity moments, the probabilities of photon-number distributions, or combinations of both. The Hillery criteria for the sums of the probabilities of even or odd photon numbers are generalized to $N$-dimensional fields. As an example, the derived nonclassicality criteria are applied to an experimental three-mode optical field containing two types of photon-pair contributions. The accompanying nonclassicality depths are used to mutually compare their performance.

## I. INTRODUCTION

Identification of nonclassicality of optical fields [1] has a long-lasting tradition in quantum optics. For many years, the nonclassicality was identified and quantified by specific physical quantities suitable for revealing the nonclassicality of different kinds of quantum fields [1]. The Fano factor that quantifies the strength of photon-number fluctuations and the principal squeeze variance [2] that measures the squeezing of field phase fluctuations serve as typical examples. With the fast development of quantum optics, a large variety of nonclassical fields has been suggested and experimentally realized [3,4]. Many of them have no distinct properties that would allow us to tailor specific nonclassicality criteria (NCCa) for them. For this reason, the NCCa started to be investigated from the general point of view.

Here, we address the NCCa based on the measurement of photon-number distributions [5] by quadratic detectors. Although these criteria are not sensitive to the phases of optical fields, they are extraordinarily useful for (spatio-spectrally) multimode optical fields. The multimode character of these fields implies that their statistical properties are fully characterized by photon-number measurements. The NCCa are traditionally written as the nonclassicality inequalities that involve the moments of integrated intensities. These integrated-intensity moments denote the normally ordered photon number moments [5] that are derived from the photon-number distributions and their usual photon-number moments with the help of the commutation relations [6]. A great deal of attention has been devoted to such NCCa for one-dimensional (1D) [7–9] and two-dimensional (2D) [10–16] optical fields for practical reasons. Among others, they allow us to identify

the nonclassicality of sub-Poissonian fields (1D) and twin beams (2D). Useful NCCa were derived by several approaches including the Cauchy-Schwarz inequality, majorization theory, and by using the classically non-negative polynomials. They were summarized in Ref. [17] for 1D and in Ref. [18] for 2D optical fields.

Klyshko suggested in Ref. [19] the use of the Mandel detection formula [1,5] in combination with the NCCa involving the intensity moments to arrive at the NCCa written in the photon-number probabilities. These criteria are in general more sensitive to the nonclassicality [20–23]. Some of them also allow us to identify the regions of photon-number distributions where the nonclassicality resides. They were extensively studied in Ref. [24] for 1D and Ref. [6] for 2D optical fields.

The 1D and 2D NCCa represent special variants of the general NCCa written for arbitrary dimensions and addressed in this paper. They are applied to marginal 1D and 2D fields of the general $N$-dimensional fields obtained by tracing out over the remaining dimensions. Thus the NCCa for dimensions greater than two are in principle more general than those written in 1D and 2D. They are indispensable for identification and quantification of the nonclassicality of fields exhibiting genuine higher-order quantum correlations. This is topical for three-dimensional (3D) fields generated in the process of third-harmonic generation (triples of photons) [25], cascaded second-order processes [26,27], or by postselection [28] (GHZ-like states).

Here, we provide the derivation of the NCCa for general $N$-dimensional optical fields by generalizing the approaches applied earlier to 1D and 2D optical fields. We reveal general relations among the derived NCCa. We show that the commonly used NCCa originating in the matrix approach using $2 \times 2$ matrices form a subset inside the group of the NCCa stemming from the Cauchy-Schwarz inequality. We

---
[*]jan.perina.jr@upol.cz

further show that the NCCa provided by the majorization theory can be decomposed into the much simpler ones. These fundamental NCCa can easily be derived by assuming simple non-negative polynomials. In general, we identify the fundamental nonclassicality inequalities, i.e., the inequalities that are not implied by other even simpler nonclassicality inequalities. We develop the approach for deriving an $N$-dimensional form of the Hillery nonclassicality criteria [29]. We also suggest a new type of the NCCa: the hybrid NCCa. They contain the field intensity moments in some dimensions while using the probabilities of photon-number distributions in the remaining dimensions.

The NCCa allow not only to identify the nonclassicality but are also useful in quantifying the nonclassicality when the Lee concept of nonclassicality depth (NCD) [30] or the nonclassicality counting parameter [31] are applied. This allows us to judge the performance of NCCa and identify the NCCa suitable for revealing the nonclassicality for given types of nonclassical states. Moreover, when a greater number of the NCCa is applied, the maximal reached NCDs are assumed to give fair estimate of the overall nonclassicality of the analyzed state. This is important in numerous applications that exploit nonclassical states.

We note that the NCCa can also be applied to optical fields that are modified before detection. This improves the ability of the NCCa to reveal the nonclassicality. Mixing of an analyzed field with a known coherent state at a beam-splitter serves as a typical example [32,33].

To demonstrate the performance of the derived NCCa, we apply the derived NCCa to a 3D optical field that is built from two photon-pair contributions. This example allows us to demonstrate the main features of the derived NCCa.

The paper is organized as follows: We bring the intensity NCCa in Sec. II whose subsections are devoted to specific kinds of the NCCa. The probability NCCa are summarized in Sec. III. Hybrid criteria are introduced in Sec. IV. The general derivation of the Hillery criteria is contained in Sec. V. Section VI is devoted to nonclassicality quantification. As an example, an experimental 3D optical field with pairwise correlations is analyzed in Sec. VII. Conclusions are drawn in Sec. VIII.

## II. INTENSITY NONCLASSICALITY CRITERIA

In this section, we pay attention to the nonclassicality inequalities that use the (integrated) intensity moments [5]. In the following sections, we apply the Cauchy-Schwarz inequality, the matrix approach, the majorization theory and the method that uses non-negative polynomials to arrive at the intensity NCCa in $N$ dimensions. We consider $N$ fields described by their intensities $W_j$ and photon numbers $n_j$, $j = 1, \ldots, N$. To formally simplify the description we write the intensities $W_j$ of the constituting fields as the elements of an $N$-dimensional intensity vector $\mathbf{W} \equiv \{W_1, \ldots, W_N\}$. Similarly, the corresponding photon numbers $n_j$ occurring in the detection of the constituting fields are conveniently arranged into a photon-number vector $\mathbf{n} \equiv \{n_1, \ldots, n_N\}$. The joint state of these fields is characterized by the joint quasidistribution $P(\mathbf{W})$ of integrated intensities and joint photon-number distribution $p(\mathbf{n})$. Intensity moments of the overall field can

then be expressed as $\langle \mathbf{W^i} \rangle \equiv \langle W_1^{i_1} \cdots W_N^{i_N} \rangle$ using the integer vector $\mathbf{i} \equiv \{i_1, \ldots, i_N\}$ containing the powers in individual dimensions. We also introduce the notation for $N$-dimensional factorial $\mathbf{i}! \equiv i_1! \ldots i_N!$.

### A. Intensity criteria based on the Cauchy-Schwarz inequality

For 2D optical fields, the Cauchy-Schwarz inequality provides a group of powerful criteria [6,23]. When we consider the real functions $f(\mathbf{W}) = \mathbf{W}^{\mathbf{l}/2+\mathbf{k}}$ and $g(\mathbf{W}) = \mathbf{W}^{\mathbf{l}/2+\mathbf{k'}}$ for arbitrary integer vectors $\mathbf{l}$, $\mathbf{k}$, and $\mathbf{k'}$, the Cauchy-Schwarz inequality $|\int f(\mathbf{W}) g(\mathbf{W}) P(\mathbf{W}) d\mathbf{W}|^2 \leqslant \int f^2(\mathbf{W}) P(\mathbf{W}) d\mathbf{W} \int g^2(\mathbf{W}) P(\mathbf{W}) d\mathbf{W}$ written for a classical non-negative probability distribution $P(\mathbf{W})$ takes the form

$$\langle \mathbf{W}^{\mathbf{l}+\mathbf{k}+\mathbf{k'}} \rangle^2 \leqslant \langle \mathbf{W}^{\mathbf{l}+2\mathbf{k}} \rangle \langle \mathbf{W}^{\mathbf{l}+2\mathbf{k'}} \rangle, \qquad (1)$$

where we use the notation $\langle \cdots \rangle = \int d\mathbf{W} P(\mathbf{W}) \cdots$ for the mean value and $d\mathbf{W} \equiv dW_1 \cdots dW_N$. Introducing the integer vectors $\mathbf{n} = \mathbf{l} + \mathbf{k} + \mathbf{k'}$ and $\mathbf{m} = \mathbf{l} + 2\mathbf{k}$ we derive the following NCCa from the classical inequality (1):

$$C_{\mathbf{n}}^{\mathbf{m}} = \langle \mathbf{W^m} \rangle \langle \mathbf{W^{2n-m}} \rangle - \langle \mathbf{W^n} \rangle^2 < 0. \qquad (2)$$

### B. Intensity criteria based on the matrix approach

Non-negative quadratic forms are conveniently written in the matrix form. Their consideration leads to powerful and versatile NCCa for 1D [17] and 2D [34–37] optical fields. Considering the determinant of the $2 \times 2$ matrix

$$\det \left\langle \begin{bmatrix} \mathbf{W^{2k}} & \mathbf{W^{k+l}} \\ \mathbf{W^{l+k}} & \mathbf{W^{2l}} \end{bmatrix} \right\rangle = \langle \mathbf{W^{2k}} \rangle \langle \mathbf{W^{2l}} \rangle - \langle \mathbf{W^{k+l}} \rangle^2 \qquad (3)$$

describing the quadratic form $(\mathbf{W^k} + \mathbf{W^l})^2$, we arrive at the NCCa that form a subset of the group $C_{\mathbf{n}}^{\mathbf{m}}$ in Eq. (2) [$\mathbf{n} \leftarrow \mathbf{k} + \mathbf{l}$, $\mathbf{m} \leftarrow 2\mathbf{l}$].

On the other hand, the quadratic form $(\mathbf{W^k} + \mathbf{W^l} + \mathbf{W^m})^2$ encoded into the $3 \times 3$ matrix

$$\begin{bmatrix} \mathbf{W^{2k}} & \mathbf{W^{k+l}} & \mathbf{W^{k+m}} \\ \mathbf{W^{l+k}} & \mathbf{W^{2l}} & \mathbf{W^{l+m}} \\ \mathbf{W^{m+k}} & \mathbf{W^{m+l}} & \mathbf{W^{2m}} \end{bmatrix} \qquad (4)$$

provides the powerful NCCa with the complex structure

$$\begin{aligned} M_{\mathbf{klm}} = &\{\langle \mathbf{W^{2k}} \rangle [\langle \mathbf{W^{2l}} \rangle \langle \mathbf{W^{2m}} \rangle - \langle \mathbf{W^{l+m}} \rangle^2] \\ &+ (\mathbf{klm}) \leftarrow (\mathbf{lmk}) + (\mathbf{klm}) \leftarrow (\mathbf{mkl})\} \\ &+ 2[\langle \mathbf{W^{k+l}} \rangle \langle \mathbf{W^{k+m}} \rangle \langle \mathbf{W^{l+m}} \rangle - \langle \mathbf{W^{2k}} \rangle \langle \mathbf{W^{2l}} \rangle \langle \mathbf{W^{2m}} \rangle] \\ &< 0. \end{aligned} \qquad (5)$$

The symbol $\leftarrow$ used in Eq. (5) stands for the terms derived from the explicitly written ones by the indicated change of indices.

### C. Intensity criteria originating in majorization theory and non-negative polynomials

In the majorization theory [38] many classical inequalities for polynomials written in fixed numbers of independent variables are derived [39]. The inequalities describing "the movement of one ball towards the right" [38] represent the basic building blocks of the remaining inequalities. Assuming the integer vectors $\mathbf{i}$ and $\mathbf{i'} = \{i_1, \ldots, i_k + 1, \ldots, i_l - $

$1, \ldots, i_N\}$, $k < l$, such that the vector $\mathbf{i}'$ majorizes the vector $\mathbf{i}$ ($\mathbf{i}' \succ \mathbf{i}$, $i_1 - 1 \geqslant i_2 - 1 \geqslant \cdots \geqslant i_{k-1} - 1 \geqslant i_k \geqslant \cdots \geqslant i_l \geqslant i_{l+1} + 1 \geqslant \cdots \geqslant i_N + 1$) they give rise to the following non-classicality inequalities:

$$\sum_{\mathcal{P}\mathbf{i}'} \langle \mathbf{W}^{\mathbf{i}'} \rangle < \sum_{\mathcal{P}\mathbf{i}} \langle \mathbf{W}^{\mathbf{i}} \rangle. \tag{6}$$

In Eq. (6), the symbol $\mathcal{P}\mathbf{i}$ stands for all permutations of the elements of vector $\mathbf{i}$.

The nonclassicality inequalities (6) can be conveniently decomposed into the much simpler ones expressed as

$$
\begin{aligned}
E_{\mathbf{i}}^{kl} = \langle \mathbf{W}^{\mathbf{i}}(W_k - W_l)^2 \rangle = \langle \mathbf{W}_{kl}^{\mathbf{i}_{kl}^{\perp}}(W_k^{i_k+2} W_l^{i_l} \\
- 2W_k^{i_k+1} W_l^{i_l+1} + W_k^{i_k} W_l^{i_l+2}) \rangle < 0;
\end{aligned} \tag{7}
$$

$\mathbf{W}_{kl} = W_1 \cdots W_{k-1} W_{k+1} \cdots W_{l-1} W_{l+1} \cdots W_N$ and $\mathbf{i}_{kl}^{\perp} = \{i_1, \ldots, i_{k-1}, i_{k+1}, \ldots, i_{l-1}, i_{l+1}, \ldots, i_N\}$. The inequality (6) can be expressed in terms of the simpler inequalities $E_{\mathbf{i}}^{kl}$ as follows ($i_k \geqslant i_l$):

$$
\begin{aligned}
\sum_{k'=1}^{N} \sum_{l'=1}^{k'-1} \sum_{\mathcal{P}\mathbf{i}_{k'l'}^{\perp}} \Big[ & E_{\mathcal{P}_{k}^{k'}\mathcal{P}_{l}^{l'}\{\ldots,i_k-1,\ldots,i_l-1,\ldots\}}^{k'l'} \\
& + E_{\mathcal{P}_{k}^{k'}\mathcal{P}_{l}^{l'}\{\ldots,i_k-2,\ldots,i_l,\ldots\}}^{k'l'} + E_{\mathcal{P}_{k}^{k'}\mathcal{P}_{l}^{l'}\{\ldots,i_k-3,\ldots,i_l+1,\ldots\}}^{k'l'} \\
& + \cdots + E_{\mathcal{P}_{k}^{k'}\mathcal{P}_{l}^{l'}\{\ldots,i_l+1,\ldots,i_k-3,\ldots\}}^{k'l'} + E_{\mathcal{P}_{k}^{k'}\mathcal{P}_{l}^{l'}\{\ldots,i_l,\ldots,i_k-2,\ldots\}}^{k'l'} \\
& + E_{\mathcal{P}_{k}^{k'}\mathcal{P}_{l}^{l'}\{\ldots,i_l-1,\ldots,i_k-1,\ldots\}}^{k'l'} \Big] < 0
\end{aligned} \tag{8}
$$

and $\mathcal{P}_k^{k'}\{\ldots, i_k, \ldots, i_{k'}, \ldots\} = \{\ldots, i_{k'}, \ldots, i_k, \ldots\}$.

As a consequence, any nonclassicality inequality stemming from the majorization theory is implied by the nonclassicality inequalities $E_{\mathbf{i}}^{kl}$ given in Eq. (7). They can simply be generalized into the NCCa

$$E_{\mathbf{i}}^{\mathbf{I}} = \left\langle \mathbf{W}^{\mathbf{i}} \prod_{k=1}^{N} \prod_{l=k+1}^{N} (W_k - W_l)^{2I_{kl}} \right\rangle < 0, \tag{9}$$

in which the integers $I_{kl}$ form an upper triangular matrix $\mathbf{I}$.

Also, other NCCa based on non-negative polynomials can be constructed. They are useful for the states with specific forms of correlations. As an example, we write the NCCa $P^k$ and $P^{kl}$,

$$P^k = \left\langle \left( \sum_{k'=1}^{N} W_{k'} - 2W_k \right)^2 \right\rangle, \tag{10}$$

$$P^{kl} = \left\langle \left( \sum_{k'=1}^{N} W_{k'} - 2W_k \right)^2 \left( \sum_{l'=1}^{N} W_{l'} - 2W_l \right)^2 \right\rangle, \tag{11}$$

which is useful for the nonclassicality analysis of the states in Sec. VI.

## III. PROBABILITY NONCLASSICALITY CRITERIA

The Mandel detection formula [1,5] written for an *N*-dimensional optical field as

$$p(\mathbf{n}) = \frac{1}{\mathbf{n}!} \int d\mathbf{W} \mathbf{W}^{\mathbf{n}} \exp(-\Sigma \mathbf{W}) P(\mathbf{W}), \tag{12}$$

with $\Sigma \mathbf{W} = \sum_{k=1}^{N} W_k$, allows us to derive the probability NCCa from the corresponding intensity NCCa according to the following mapping (for details, see the next section):

$$\mathbf{W}^{\mathbf{n}} \leftarrow \mathbf{n}! \, p(\mathbf{n})/p(\mathbf{0}), \tag{13}$$

where the symbol $\mathbf{0}$ denotes the vector with all elements equal to zero.

Using the mapping (13), the intensity NCCa $C_{\mathbf{n}}^{\mathbf{m}}$ from Eq. (3) derived from the Cauchy-Schwarz inequality give the following probability NCCa:

$$\bar{C}_{\mathbf{n}}^{\mathbf{m}} = \frac{(2\mathbf{n} - \mathbf{m})! \mathbf{m}!}{(\mathbf{n}!)^2} p(\mathbf{m}) p(2\mathbf{n} - \mathbf{m}) - p^2(\mathbf{n}) < 0. \tag{14}$$

Similarly, the intensity NCCa $M_{\mathbf{klm}}$ in Eq. (5) obtained by the matrix approach are transformed into the following probability NCCa:

$$
\begin{aligned}
\bar{M}_{\mathbf{klm}} = \Bigg\{ & p(2\mathbf{k}) \bigg[ p(2\mathbf{l}) p(2\mathbf{m}) - \frac{(\mathbf{l} + \mathbf{m})!^2}{(2\mathbf{l})!(2\mathbf{m})!} p^2(\mathbf{l} + \mathbf{m}) \bigg] \\
& + (\mathbf{klm}) \leftarrow (\mathbf{mkl}) + (\mathbf{klm}) \leftarrow (\mathbf{lmk}) \Bigg\} \\
& + 2 \bigg[ \frac{(\mathbf{k} + \mathbf{l})!(\mathbf{k} + \mathbf{m})!(\mathbf{l} + \mathbf{m})!}{(2\mathbf{k})!(2\mathbf{l})!(2\mathbf{m})!} p(\mathbf{k} + \mathbf{l}) p(\mathbf{k} + \mathbf{m}) \\
& \times p(\mathbf{l} + \mathbf{m}) - p(2\mathbf{k}) p(2\mathbf{l}) p(2\mathbf{m}) \bigg] < 0. 
\end{aligned} \tag{15}
$$

Finally, the NCCa $E_{\mathbf{i}}^{kl}$ from Eq. (7) give rise to the following probability NCCa:

$$
\begin{aligned}
\bar{E}_{\mathbf{i}}^{kl} = & (i_k + 2)(i_k + 1) p(\ldots, i_k + 2, \ldots, i_l, \ldots) \\
& + (i_l + 2)(i_l + 1) p(\ldots, i_k, \ldots, i_l + 2, \ldots) \\
& - 2(i_k + 1)(i_l + 1) p(\ldots, i_k + 1, \ldots, i_l + 1, \ldots) < 0.
\end{aligned} \tag{16}
$$

## IV. HYBRID NONCLASSICALITY CRITERIA

In general, via the mapping in Eq. (13), we may map the intensity moments to the probabilities only in some dimensions. This leads to hybrid NCCa that combine the intensity moments and probabilities. This results in the use of "mixed moments" that are determined by using the formula

$$
\begin{aligned}
\langle \mathbf{W}_W^{\mathbf{i}_W} \rangle_{p_p(\mathbf{i}_p)} = & \int d\mathbf{W}_W \mathbf{W}_W^{\mathbf{i}_W} \frac{1}{\mathbf{i}_p!} \int d\mathbf{W}_p \mathbf{W}_p^{\mathbf{i}_p} \\
& \times \exp(-\Sigma \mathbf{W}_p) P(\mathbf{W}_W, \mathbf{W}_p),
\end{aligned} \tag{17}
$$

in which we split the elements of integer vector $\mathbf{i}$ describing the intensity-moment powers into two groups. In Eq. (17), we denote the corresponding integer vectors by $\mathbf{i}_W$ and $\mathbf{i}_p$ and the corresponding intensities by $\mathbf{W}_W$ and $\mathbf{W}_p$.

To reveal the mapping between the intensity and probability NCCa, let us consider the normalized distribution $P'(\mathbf{W}_W, \mathbf{W}_p) = \exp(-\Sigma \mathbf{W}_p) P(\mathbf{W}_W, \mathbf{W}_p)/[\int d\mathbf{W}_W' \int d\mathbf{W}_p' \exp(-\Sigma \mathbf{W}_p') P(\mathbf{W}_W', \mathbf{W}_p')]$ that stays non-negative provided that the original distribution $P(\mathbf{W}_W, \mathbf{W}_p)$ is non-negative. Thus the moments $\langle\langle \mathbf{W}_W^{\mathbf{i}_W} \mathbf{W}_p^{\mathbf{i}_p} \rangle\rangle$ of this distribution,

$$
\begin{aligned}
\langle\langle \mathbf{W}_W^{\mathbf{i}_W} \mathbf{W}_p^{\mathbf{i}_p} \rangle\rangle = & \int d\mathbf{W}_W \int d\mathbf{W}_p \mathbf{W}_W^{\mathbf{i}_W} \mathbf{W}_p^{\mathbf{i}_p} \\
& \times P'(\mathbf{W}_W, \mathbf{W}_p),
\end{aligned} \tag{18}
$$

when substituted into the nonclassicality inequalities with intensity moments in Sec. II, give rise to the NCCa. When we express these NCCa in terms of the mixed moments defined in Eq. (17), we reveal the following mapping:

$$\mathbf{W}_W^{\mathbf{i}_W} \mathbf{W}_P^{\mathbf{i}_p} \leftarrow \mathbf{W}_W^{\mathbf{i}_W} \mathbf{i}_p! \, p_p(\mathbf{i}_p)/p_p(\mathbf{0}) \qquad (19)$$

in which the marginal photon-number distribution $p_p$ is defined in the dimensions grouped into the integer vector $\mathbf{i}_p$:

$$p_p(\mathbf{i}_p) = \frac{1}{\mathbf{i}_p!} \int d\mathbf{W}_p \mathbf{W}_p^{\mathbf{i}_p} \exp\left(-\Sigma \mathbf{W}_p\right)$$
$$\times \int d\mathbf{W}_W P(\mathbf{W}_W, \mathbf{W}_p). \qquad (20)$$

As an example of mapping in Eq. (19), we write the hybrid NCCa derived from the intensity NCCa in Eq. (2) that originate in the Cauchy-Schwarz inequality:

$$\tilde{C}_{\mathbf{n}_W,\mathbf{n}_p}^{\mathbf{m}_W,\mathbf{m}_p} = \frac{(2\mathbf{n}_p - \mathbf{m}_p)! \mathbf{m}_p!}{(\mathbf{n}_p!)^2} \langle \mathbf{W}_W^{2\mathbf{n}_W - \mathbf{m}_W} \rangle_{p_p(2\mathbf{n}_p - \mathbf{m}_p)}$$
$$\times \langle \mathbf{W}_W^{\mathbf{m}_W} \rangle_{p_p(\mathbf{m}_p)} - \langle \mathbf{W}_W^{\mathbf{n}_W} \rangle_{p_p(\mathbf{n}_p)}^2 < 0, \qquad (21)$$

where the hybrid moments are determined by using Eq. (17).

## V. GENERALIZED HILLERY NONCLASSICALITY CRITERIA

The Hillery NCCa were derived for the sums of probabilities of even and odd photon numbers for 1D optical fields [29]. They are suitable, e.g., for evidencing the nonclassicality of single-mode squeezed-vacuum states.

To reveal their $N$-dimensional generalizations, we first consider the following classical inequality:

$$\int d\mathbf{W} \, \mathrm{ch}(W_+) \exp\left(-W_+\right) P(\mathbf{W}) \geqslant 1/2, \qquad (22)$$

valid for any classical non-negative distribution $P(\mathbf{W})$. In Eq. (22), ch stands for the hyperbolic cosine and $W_+ = \Sigma \mathbf{W}$. A suitable unitary transformation to new variables that involves the variable $W_+$ and replacement of ch function by the defining exponentials immediately reveal the inequality (22). The Taylor expansion of the ch function and the use of multinomial expansion transform the inequality (22) into the form:

$$\sum_{l=0}^{\infty} \sum_{\mathbf{n}=\mathbf{0}, \sum \mathbf{n}=2l}^{\infty} \frac{1}{\mathbf{n}!} \int d\mathbf{W} \, \mathbf{W}^{\mathbf{n}} \exp\left(-W_+\right) P(\mathbf{W}) \geqslant 1/2. \quad (23)$$

The comparison of integrals in Eq. (23) with the Mandel detection formula (12) results in the following generalized Hillery NCC $H_1$ for the probabilities of even-summmed photon numbers:

$$H_1 = \sum_{l=0}^{\infty} \sum_{\mathbf{n}=\mathbf{0}, \sum \mathbf{n}=2l}^{\infty} p(\mathbf{n}) - 1/2 < 0. \qquad (24)$$

The second Hillery NCC is obtained starting from the classical inequality

$$\int d\mathbf{W} \, [\mathrm{sh}(W_+) - \mathrm{ch}(W_+) + 1] \exp\left(-W_+\right) P(\mathbf{W}) \geqslant 0, \quad (25)$$

in which sh denotes the hyperbolic sine. Similarly as above, the use of the Taylor expansion for sh and ch functions, multinomial expansion, and the Mandel detection formula leaves us with the following NCC:

$$\sum_{l=0}^{\infty} \sum_{\mathbf{n}=\mathbf{0}, \sum \mathbf{n}=1+2l}^{\infty} p(\mathbf{n}) - \sum_{l=0}^{\infty} \sum_{\mathbf{n}=\mathbf{0}, \sum \mathbf{n}=2l}^{\infty} p(\mathbf{n}) + p(\mathbf{0}) < 0. \qquad (26)$$

The use of the normalization condition $\sum_{\mathbf{n}=\mathbf{0}}^{\infty} p(\mathbf{n}) = 1$ in Eq. (26) leads to the second generalized Hillery NCC $H_2$ for the probabilities of odd-summed photon numbers:

$$H_2 = \sum_{l=0}^{\infty} \sum_{\mathbf{n}=\mathbf{0}, \sum \mathbf{n}=1+2l}^{\infty} p(\mathbf{n}) - [1 - p(\mathbf{0})]/2 < 0. \qquad (27)$$

## VI. QUANTIFICATION OF NONCLASSICALITY

The above written NCCa can be used not only as nonclassicality identifiers. When we apply the concept of the Lee nonclassicality depth [30], they also quantitatively characterize the nonclassicality. This quantification is based upon the properties of optical fields described in different field-operator orderings [5]. Whereas the normally ordered intensity moments contain only the intrinsic noise of the field, the general $s$-ordered intensity moments involve an additional "detection" thermal noise with the mean photon number $(1 - s)/2$ per one mode [5,30]. Such noise gradually decreases the nonclassicality as the ordering parameter $s$ decreases. The threshold value $s_{\mathrm{th}}$ at which a given field loses its nonclassicality then determines the nonclassicality depth (NCD) $\tau$ [30]:

$$\tau = \frac{1 - s_{\mathrm{th}}}{2}. \qquad (28)$$

We note that, alternatively, we may apply the nonclassicality counting parameter introduced in Ref. [31].

To arrive at the NCDs $\tau$ of the above written NCCa, we have to transform the mixed moments $\langle \mathbf{W}_W^{\mathbf{i}_W} \rangle_{p_p(\mathbf{i}_p)}$ of Eq. (17) to their general $s$-ordered form $\langle \mathbf{W}_W^{\mathbf{i}_W} \rangle_{p_p(\mathbf{i}_p),s}$. Using the results of Refs. [5,6], the corresponding transformation is accomplished via the matrices $S_W$ and $S_p$ appropriate to the intensity moments and probabilities, respectively,

$$\langle \mathbf{W}_W^{\mathbf{i}_W} \rangle_{p_p(\mathbf{i}_p),s} = \sum_{\mathbf{i}_W'=\mathbf{1}}^{\mathbf{i}_W} S_W\left(i_{1_W}, i_{1_W}'; s, M_{1_W}\right) \cdots$$
$$S_W\left(i_{N_W}, i_{N_W}'; s, M_{N_W}\right) \sum_{\mathbf{i}_p'=\mathbf{0}}^{\infty} S_p\left(i_{1_p}, i_{1_p}'; s, M_{1_p}\right)$$
$$\cdots S_p\left(i_{N_p}, i_{N_p}'; s, M_{N_p}\right) \langle \mathbf{W}_W^{\mathbf{i}_W} \rangle_{p_p(\mathbf{i}_p')}, \qquad (29)$$

$\mathbf{1} \equiv \{1, 1, \ldots\}$ and integer vectors $\mathbf{M}_W \equiv \{M_{1_W}, \ldots, M_{N_W}\}$ and $\mathbf{M}_p \equiv \{M_{1_p}, \ldots, M_{N_p}\}$ give the numbers of modes in all dimensions of the analyzed optical field. In Eq. (29), the transformation matrices $S_W$ and $S_p$ are defined as follows:

$$S_W(i, i'; s, M) = \binom{i}{i'} \frac{\Gamma(i + M)}{\Gamma(i' + M)} \left(\frac{1 - s}{2}\right)^{i - i'}, \qquad (30)$$
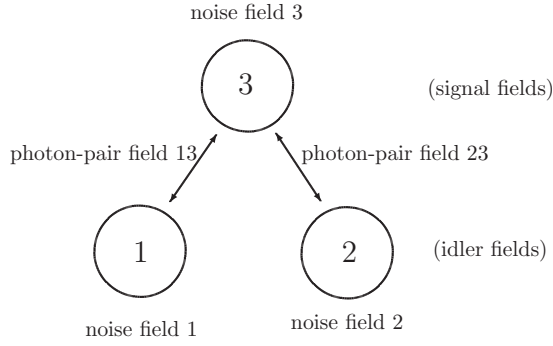
FIG. 1. Structure of the analyzed 3D optical field composed of ideal photon-pair fields 13 and 23 and noise fields 1, 2, and 3.

$$S_p(i, i'; s, M) = \left(\frac{2}{3-s}\right)^M \left(\frac{1+s}{1-s}\right)^{i'} \left(\frac{1-s}{3-s}\right)^i$$
$$\times \sum_{l=0}^{i'} (-1)^{i'-l} \binom{i'}{l} \binom{i+l+M-1}{i}$$
$$\times \left(\frac{4}{(1+s)(3-s)}\right)^l. \tag{31}$$

## VII. APPLICATION OF THE DERIVED NONCLASSICALITY CRITERIA TO A THREE-DIMENSIONAL OPTICAL FIELD

We demonstrate the performance of the above written NCCa in revealing the nonclassicality using a 3D optical field containing two types of photon pairs. This 3D field was generated in the pulsed multimode spontaneous parametric down-conversion from two nonlinear crystals that produced two types of photon pairs differing in polarization (for details, see Ref. [15]). While the idler fields constitute fields 1 and 2, the signal fields overlap in a common detection area and together form field 3, as schematically shown in Fig. 1. The experimental photocount histogram $f(c_1, c_2, c_3)$ that gives the normalized number of simultaneous detections of $c_i$ photocounts in field $i$, $i = 1, 2, 3$, in $1.2 \times 10^6$ measurements [15] was reconstructed by using the maximum likelihood (ML) approach [40,41]. The iteration algorithm ($j$ numbers the iteration steps)

$$p^{(j+1)}(\mathbf{n}) = \sum_{\mathbf{c}=\mathbf{0}}^{\infty} \frac{f(\mathbf{c}) T(\mathbf{c}, \mathbf{n})}{\sum_{\mathbf{n}'=\mathbf{0}}^{\infty} T(\mathbf{c}, \mathbf{n}') p^{(j)}(\mathbf{n}')} \tag{32}$$

provided the reconstructed 3D photon-number distribution $p(n_1, n_2, n_3)$ that we analyze below from the point of view of its nonclassicality. In Eq. (32), the detection function $T(\mathbf{c}, \mathbf{n})$ gives the probability of detecting $\mathbf{c}$ photocounts at $N$ detectors being illuminated by $\mathbf{n}$ photons. The theoretical prediction $f^{\text{th}}(\mathbf{c})$ for the photocount histogram is obtained as $f^{\text{th}}(\mathbf{c}) = \sum_{\mathbf{n}=\mathbf{0}}^{\infty} T(\mathbf{c}, \mathbf{n}) p(\mathbf{n})$. The analyzed photon-number distribution $p$ is shown in Fig. 2 in two characteristic cuts suitable for visualization of its pairwise structure.

The experimental 3D optical field was also fit by the model of two ideal multimode Gaussian twin beams ($6.15 \pm 0.05$ and $5.95 \pm 0.05$ mean photon pairs) and three multimode
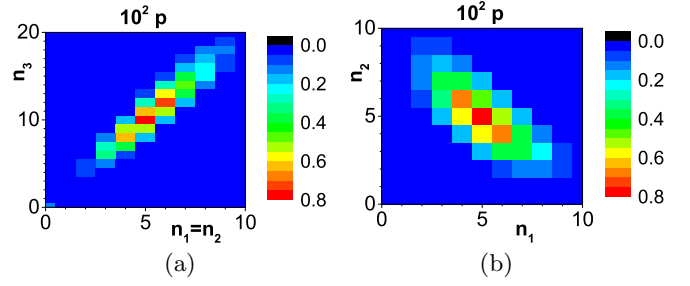


FIG. 2. Photon-number distribution $p(n_1, n_2, n_3)$ obtained by ML approach in 2D cuts: (a) $p(n_1 = n_2, n_3)$ and (b) $p(n_1, n_2, n_3 = 10)$. Relative errors are better than 1%.

Gaussian noise fields ($0.11 \pm 0.02$, $0.07 \pm 0.01$, and $0.02 \pm 0.01$ mean noise photons). Details are found in Ref. [15].

By definition, the nonclassicality of an optical field means that its quasidistributions $P_W$ of integrated intensities attain negative values for ordering parameters $s > s_{\text{th}}$ where $s_{\text{th}}$ denotes a threshold value of the ordering parameter. An $s$-ordered quasidistribution $P_{W,s}(\mathbf{W})$ of integrated intensities for one effective mode in each field is obtained by the following formula [5]:

$$P_{W,s}(\mathbf{W}) = \frac{2^N}{(1-s)^N} \exp\left(-\frac{2\Sigma\mathbf{W}}{1-s}\right) \sum_{\mathbf{n}=\mathbf{0}}^{\infty} \frac{p(\mathbf{n})}{\mathbf{n}!}$$
$$\times \left(\frac{s+1}{s-1}\right)^{\Sigma\mathbf{n}} L_{n_1}\left(\frac{4W_1}{1-s^2}\right) \cdots L_{n_N}\left(\frac{4W_N}{1-s^2}\right), \tag{33}$$

where $L_k$ stand for the Laguerre polynomials [42]. We demonstrate the nonclassical behavior of quasidistribution $P_W$ in Fig. 3 where we plot two characteristic cuts for $s = 0.02$. Whereas the quasidistribution $P_W$ creates hyperbolic structures in planes $(W_1, W_2)$ (for fixed values of intensity $W_3$), it forms the structure of rays coming from the point $(W_1, W_2, W_3) = (0, 0, 0)$ in plane $(W_1 = W_2, W_3)$ that is well known for twin beams [18].

Now we apply the appropriate NCCa of Sec. II for the introduced $N = 3$ dimensional optical field. We address in turn intensity NCCa, probability NCCa and hybrid NCCa.
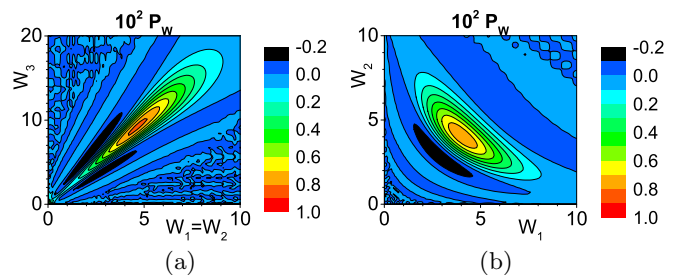


FIG. 3. Quasidistribution $P_W(W_1, W_2, W_3)$ of integrated intensities for the ordering parameter $s = 0.02$ and the field obtained by ML approach in 2D cuts: (a) $P_W(W_1 = W_2, W_3)$ and (b) $P_W(W_1, W_2, W_3 = 7.9)$.
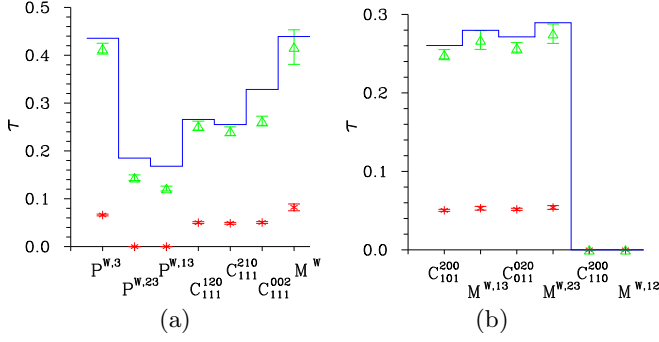
FIG. 4. Nonclassicality depths $\tau$ for (a) 3D and (b) 2D intensity NCCa. Isolated symbols with error bars are drawn for the experimental photocount histogram (red $*$) and field reconstructed by ML approach (green $\triangle$); solid blue curves originate in 3D Gaussian model.

### A. Application of intensity nonclassicality criteria

The intensity NCCa containing the lower-order intensity moments are in general stable when applied to the experimental data. This is a consequence of the fact that all experimental data are exploited when the intensity moments are determined. This contrasts with the probability NCCa where only a rather limited amount of the experimental data is used for each NCC. It holds in general for the intensity NCCa that the greater the order of the moments used in a given NCC is the greater the experimental error is. Nevertheless, the NCCa containing the lowest-order intensity moments are usually reliable and very efficient in revealing the nonclassicality.

The following intensity NCCa (arranged according to the increasing order of involved intensity moments) derived from the general ones in Eqs. (2), (5) [assuming $\mathbf{k} = (1, 0, 0)$, $\mathbf{l} = (0, 1, 0)$, $\mathbf{m} = (0, 0, 1)$], (10), and (11) are capable of identifying the nonclassicality of the analyzed field:

$$P^{W,3} = \langle (W_1 + W_2 - W_3)^2 \rangle < 0,$$
$$P^{W,13} = \langle (-W_1 + W_2 + W_3)^2 (W_1 + W_2 - W_3)^2 \rangle < 0,$$
$$P^{W,23} = \langle (W_1 - W_2 + W_3)^2 (W_1 + W_2 - W_3)^2 \rangle < 0,$$
$$C_{111}^{120} = \langle W_1 W_2^2 \rangle \langle W_1 W_3^2 \rangle - \langle W_1 W_2 W_3 \rangle^2 < 0,$$
$$C_{111}^{210} = \langle W_1^2 W_2 \rangle \langle W_2 W_3^2 \rangle - \langle W_1 W_2 W_3 \rangle^2 < 0,$$
$$C_{111}^{002} = \langle W_1^2 W_2^2 \rangle \langle W_3^2 \rangle - \langle W_1 W_2 W_3 \rangle^2 < 0,$$
$$M^W = \langle W_1^2 \rangle \langle W_2^2 \rangle \langle W_3^2 \rangle + \langle W_1 W_2 \rangle \langle W_1 W_3 \rangle \langle W_2 W_3 \rangle$$
$$- \langle W_1^2 \rangle \langle W_2 W_3 \rangle^2 - \langle W_2^2 \rangle \langle W_1 W_3 \rangle^2$$
$$- \langle W_3^2 \rangle \langle W_1 W_2 \rangle^2. \tag{34}$$

The polynomial NCC $P^{W,3}$ and the matrix NCC $M^W$ provide the greatest values of their NCDs $\tau$ around 0.4, as follows from the graph in Fig. 4(a). Whereas the matrix NCCa with their complex moment structures are in general successful in revealing the nonclassicality, the simple polynomial NCC $P^{W,3}$ complies with the pairwise structure of the analyzed field. The specific type of pairwise correlations in the analyzed field is also detected by the fourth-order Cauchy-Schwarz NCCa $C_{111}^{120}$, $C_{111}^{210}$, and $C_{111}^{002}$ though the values of

the corresponding NCDs $\tau$ are smaller. Also the fourth-order polynomial NCCa $P^{W,13}$ and $P^{W,23}$ reveal the nonclassicality, owing to the involved term $(W_1 + W_2 - W_3)^2$ that they share with the powerful NCC $P^{W,3}$.

More detailed information about the structure of correlations in the analyzed field is obtained when the marginal intensity quasidistributions are analyzed. The following fourth-order intensity NCCa derived from Eqs. (2) and (5) [assuming $\mathbf{k} = (0, 0)$, $\mathbf{l} = (1, 0)$, $\mathbf{m} = (0, 1)$] were found useful for this task:

$$C_{101}^{200} = \langle W_1^2 \rangle \langle W_3^2 \rangle - \langle W_1 W_3 \rangle^2 < 0,$$
$$C_{110}^{200} = \langle W_1^2 \rangle \langle W_2^2 \rangle - \langle W_1 W_2 \rangle^2 < 0,$$
$$C_{011}^{020} = \langle W_2^2 \rangle \langle W_3^2 \rangle - \langle W_2 W_3 \rangle^2 < 0,$$
$$M^{W,ij} = \langle W_i^2 \rangle \langle W_j^2 \rangle + 2\langle W_i \rangle \langle W_j \rangle \langle W_i W_j \rangle$$
$$- \langle W_i \rangle^2 \langle W_j^2 \rangle - \langle W_i^2 \rangle \langle W_j \rangle^2 - \langle W_i W_j \rangle^2,$$
$$(i, j) = (1, 2), (1, 3)(2, 3). \tag{35}$$

The corresponding NCDs $\tau$ are shown in Fig. 4(b). They reveal strong correlations in the marginal fields (1,3) and (2,3) and no correlation in the marginal field (1,2), in agreement with the structure of the experimentally generated 3D field. Both the matrix and the Cauchy-Schwarz NCCa lead to the values of NCDs $\tau$ around 0.25 for the fields (1,3) and (2,3). The NCDs $\tau$ shown in Fig. 4 indicate slightly greater nonclassicality in the field (2,3) compared with the field (1,3).

The values of NCDs $\tau$ in Fig. 4 determined for the model Gaussian field (solid blue curves) are slightly greater than those obtained for the analyzed field reconstructed by the ML approach (green $\triangle$). This reflects the fact that the Gaussian model partly conceals the noise present in the experimental data. For comparison, we plot in Fig. 4 also the values of the NCDs $\tau$ determined directly from the experimental photocount histogram $f$ (red $*$). Whereas the NCCa $P^{W,3}$ and $M^W$ give the greatest values of NCDs $\tau$ already for the histogram $f$, the NCCa $P^{W,13}$ and $P^{W,23}$ do not indicate the nonclassicality in the histogram $f$; they need stronger and less-noisy fields for successful application.

### B. Probability nonclassicality criteria

In general, the probability NCCa are more efficient in revealing the nonclassicality [23,24] compared with their intensity counterparts. The reason is that they test the field nonclassicality locally via the probabilities in the field photon-number distribution. On the other hand, the determination of probabilities is more prone to experimental errors compared with the intensity moments whose determination involves all probabilities.

Local nonclassicality can be investigated by using suitable probability NCCa containing only the probabilities from small regions. We illustrate this approach by defining the probability NCCa $C^p$ and $M^p$ that are in fact specific groups of the Cauchy-Schwarz and the matrix NCCa from Eqs. (14) and (15):

$$C_{\mathbf{n}}^p = \min_{\mathbf{m}, |\mathbf{m}-\mathbf{n}| \leqslant 1} \{\bar{C}_{\mathbf{n}}^{\mathbf{m}}\} < 0,$$
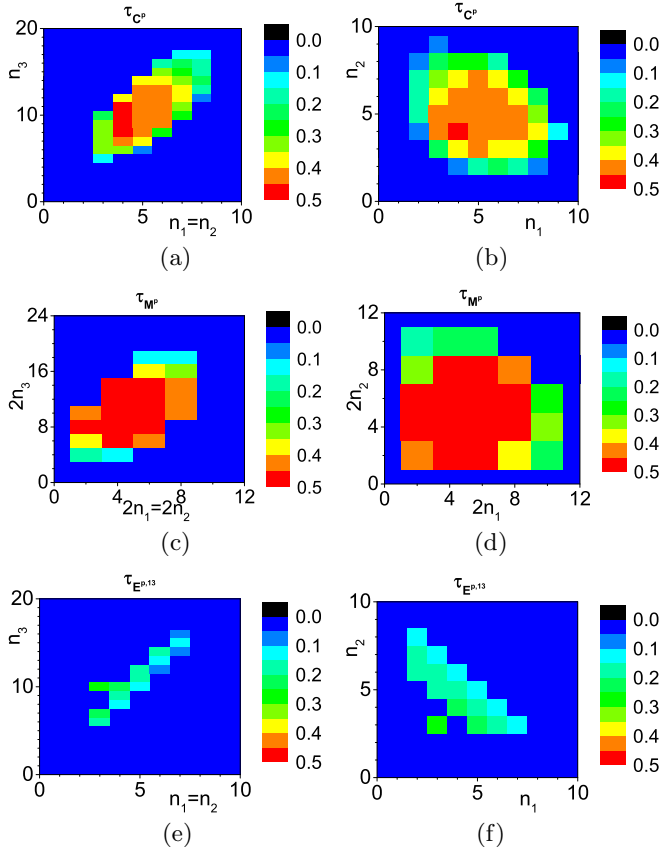
FIG. 5. Nonclassicality depths $\tau$ for probability NCCa (a), (b) $C^p$, (c), (d) $M^p$, and (e), (f) $E^{p,13}$ as they depend on photon numbers $n_1$, $n_2$, and $n_3$ in 2D cuts; $n_3 = 10$ in panels (b) and (f), $2n_3 = 10$ in panel (d). Only the NCCa for which the mean value of the used probabilities is greater than 0.001 are taken into account. Relative errors in panels (a), (b); (c), (d); and (e), (f) are in turn better than 3%, 8%, and 2%, respectively.

$$M_{\mathbf{n}}^p = \min_{\mathbf{k},\mathbf{l},|\mathbf{k}-\mathbf{n}|\leqslant 1,|\mathbf{l}-\mathbf{n}|\leqslant 1}\{\bar{M}_{\mathbf{kln}}\} < 0, \qquad (36)$$

where $|\mathbf{m}-\mathbf{n}| \leqslant 1$ stands for the simultaneous conditions $|m_i - n_i| \leqslant 1$ for $i = 1, 2, 3$. We also consider the probability polynomial NCCa $E^{p,13}$ derived from the intensity NCCa in Eq. (7) because these NCCa are efficient in identifying the nonclassicality originating in photon pairing [6]:

$$E_{\mathbf{n}}^{p,13} = \frac{n_1 + 2}{n_3 + 1}p(n_1 + 2, n_2, n_3) + \frac{n_3 + 2}{n_1 + 1}p(n_1, n_2, n_3 + 2)$$
$$- 2p(n_1 + 1, n_2, n_3 + 1) < 0. \qquad (37)$$

The cuts of the probability NCCa $C^p$, $M^p$, and $E^{p,13}$ plotted in Fig. 5, which correspond to the cuts of the photon-number distribution $p$ in Fig. 2, reveal that the greatest values of the NCDs $\tau$ occur in the central part of the 3D photon-number distribution $p$. These values drop down as we move towards the photon-number distribution tails. As documented in the graphs of Fig. 5 the matrix NCCa $M^p$ perform the best followed by the Cauchy-Schwarz NCCa $C^p$; both types of NCCa indicate the greatest values of NCDs $\tau$ close to 0.5. The polynomial NCCa $E^{p,13}$ give the maximal values of NCDs $\tau$ only around 0.3, which is a consequence of their structure

that is sensitive only to photon pairs in the field 13. Comparing the probability NCCa with their intensity counterparts, the NCDs $\tau$ are greater by around 0.1 (0.2) for the matrix (Cauchy-Schwarz) NCCa.

Contrary to the probability NCCa discussed above and containing finite numbers of probabilities, the Hillery criteria $H_1$ and $H_2$ from Eqs. (24) and (27) contain infinite numbers of probabilities. However, they did not perform well when analyzing the 3D field reconstructed by the ML approach: Only the NCC $H_2$ applied in 3D provided a nonzero value of NCD $\tau = 0.020 \pm 0.001$. On the other hand, for the model Gaussian field, the NCCa $H_2$ revealed the nonclassicality of 3D field ($\tau = 0.211$) as well as the marginal 2D fields (1,3) ($\tau = 0.015$) and (2,3) ($\tau = 0.050$). This indicates that the Hillery criteria are not suitable for identifying the nonclassicality in experimental photon-number distributions because of the inevitable noise.

### C. Hybrid nonclassicality criteria

The hybrid criteria that contain both probabilities and intensity moments represent in a certain sense a bridge between the intensity and probability NCCa. Their expected performance in revealing the nonclassicality and resistance against the experimental errors lie in the middle. On one side they are less efficient but more stable than the probability NCCa, on the other side they are more powerful but less stable than the intensity NCCa. With their help, we can monitor specific aspects of the nonclassicality of the analyzed fields including the experimental issues.

To demonstrate their properties, we first consider the following Cauchy-Schwarz and the matrix NCCa derived from Eq. (21) [assuming $\mathbf{m}_W = (0, 2)$, $\mathbf{n}_W = (1, 1)$, $\mathbf{m}_p = (n_k - m_k)$, $\mathbf{n}_p = (n_k)$] and Eq. (5) converted partly into the probability NCCa via the mapping in Eq. (19) [assuming $\mathbf{k} = (0, 0, n_k)$, $\mathbf{l} = (1, 0, n_k)$, $\mathbf{m} = (0, 1, n_k)$]:

$$C_{n_k,m_k}^{pW,k} = \frac{(n_k + m_k)!(n_k - m_k)!}{(n_k!)^2}\langle W_i^2\rangle_{p_k(n_k+m_k)}$$
$$\times \langle W_j^2\rangle_{p_k(n_k-m_k)} - \langle W_i W_j\rangle_{p_k(n_k)}^2 < 0,$$

$$M_{n_k}^{pW,k} = \langle 1\rangle_{p_k(2n_k)}\langle W_i^2\rangle_{p_k(2n_k)}\langle W_j^2\rangle_{p_k(2n_k)}$$
$$+ 2\langle W_i\rangle_{p_k(2n_k)}\langle W_j\rangle_{p_k(2n_k)}\langle W_i W_j\rangle_{p_k(2n_k)}$$
$$- \langle W_i\rangle_{p_k(2n_k)}^2\langle W_j^2\rangle_{p_k(2n_k)} - \langle W_i^2\rangle_{p_k(2n_k)}\langle W_j\rangle_{p_k(2n_k)}^2$$
$$- \langle 1\rangle_{p_k(2n_k)}\langle W_i W_j\rangle_{p_k(2n_k)}^2 < 0,$$

$$(i, j, k) = (1, 2, 3), \ (2, 3, 1), \ (3, 1, 2). \qquad (38)$$

The Cauchy-Schwarz NCC $C^{pW,k}$ for $m_k = 0$ represents a 2D intensity NCC for the field $(i, j)$ conditioned by the detection of $n_k$ photons in field $k$. The values of NCDs $\tau$ for the field (2,3) lie around 0.35, as documented in Fig. 6(a). They are greater by around 0.1 compared with the value $\tau = 0.257 \pm 0.007$ for the NCC $C_{011}^{020}$ of the marginal field (2,3). This is explained as follows: The conditional fields occur in the decomposition of the marginal field (2,3) (with appropriate weights). Composing the marginal field from its conditional constituents we partly conceal the nonclassical-
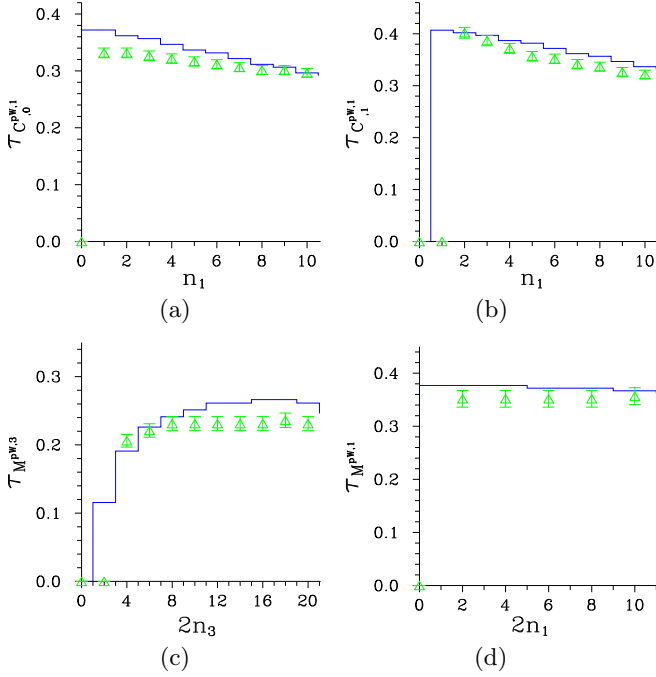
FIG. 6. Nonclassicality depths $\tau$ for hybrid NCCa (a) $C_{,0}^{pW,1}$, (b) $C_{,1}^{pW,1}$, (c) $M^{pW,3}$, and (d) $M^{pW,1}$ as they depend on the corresponding photon numbers $n_1$, $2n_1$, and $2n_3$. Isolated symbols with error bars are plotted for the field reconstructed by ML approach (green $\triangle$); solid blue curves originate in 3D Gaussian model.

ity. The Cauchy-Schwarz NCC $C^{pW,k}$ in its general form ($m_k \neq 0$) involves the moments of three 2D fields $(i, j)$ conditioned by the detection of $n_k - m_k$, $n_k$, and $n_k + m_k$ photons in field $k$. In its general form it allows us to reach even greater values of the NCDs $\tau$, as demonstrated in Fig. 6(b).

Two limiting cases of the behavior of the nonclassicality when composing the field from its conditional constituents are shown in Figs. 6(c) and 6(d) considering the matrix NCCa $M^{pW,1}$ and $M^{pW,3}$ from Eq. (36). Whereas the hybrid NCCa $M^{pW,3}$ indicate the NCDs $\tau$ around 0.22 for the conditional fields (1,2) in Fig. 6(c), the marginal field (1,2) is classical ($M^{W,23} = 0$). On the other hand, the hybrid NCCa $M^{pW,1}$ assign the NCDs $\tau$ around 0.35 for the conditional fields (2,3) and similar value $\tau = 0.28 \pm 0.01$ is obtained for the marginal field (2,3) applying the NCC $M^{W,23}$. We note that, in Fig. 6, similarly as in the case of intensity NCCa, the values of NCDs $\tau$ obtained from the model Gaussian field are slightly greater than those characterizing the field reconstructed by the ML approach.

As another example, we consider the following hybrid Cauchy-Schwarz and matrix criteria $C^{Wp,i}$ and $M^{Wp,i}$ obtained from Eq. (21) [assuming $\mathbf{m}_W = (0)$, $\mathbf{n}_W = (1)$, $\mathbf{m}_p = \mathbf{n}_p = (n_j, n_k)$] and Eq. (5) converted into the probability NCCa [assuming $\mathbf{k} = (0, n_j, n_k)$, $\mathbf{l} = (1, n_j, n_k)$, $\mathbf{m} = (2, n_j, n_k)$] using the mapping in Eq. (19):

$$C_{n_j, n_k}^{Wp,i} = \langle W_i^2 \rangle_{p_{jk}(n_j, n_k)} \langle 1 \rangle_{p_{jk}(n_j, n_k)} - \langle W_i \rangle_{p_{jk}(n_j, n_k)}^2 < 0,$$

$$M_{n_j, n_k}^{Wp,i} = \langle 1 \rangle_{p_{jk}(2n_j, 2n_k)} \langle W_i^2 \rangle_{p_{jk}(2n_j, 2n_k)} \langle W_i^4 \rangle_{p_{jk}(2n_j, 2n_k)}$$
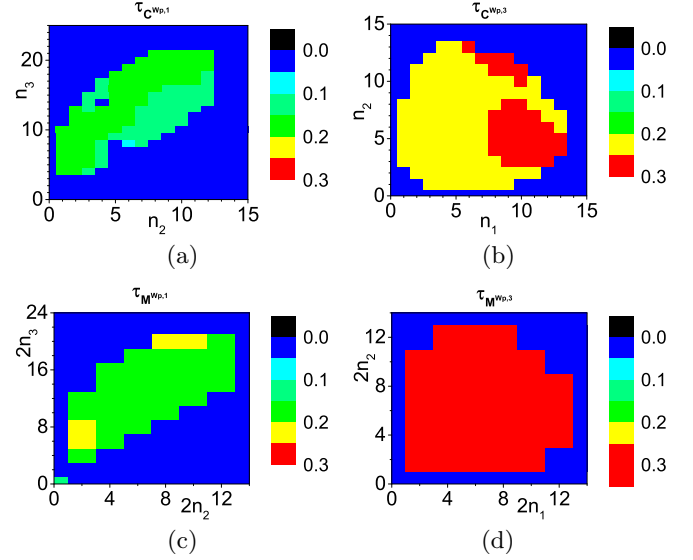


FIG. 7. Nonclassicality depths $\tau$ for hybrid NCCa (a) $C^{Wp,1}$, (b) $C^{Wp,3}$, (c) $M^{Wp,1}$, and (d) $M^{Wp,3}$ as they depend on the corresponding photon numbers $n_1$, $n_2$, $n_3$, $2n_1$, $2n_2$, and $2n_3$. Relative errors in panels (a) and (b) [(c) and (d)] are better than 3% (15%).

$$+ 2\langle W_i \rangle_{p_{jk}(2n_j, 2n_k)} \langle W_i^2 \rangle_{p_{jk}(2n_j, 2n_k)} \langle W_i^3 \rangle_{p_{jk}(2n_j, 2n_k)}$$

$$- \langle 1 \rangle_{p_{jk}(2n_j, 2n_k)} \langle W_i^3 \rangle_{p_{jk}(2n_j, 2n_k)}^2 - \langle W_i \rangle_{p_{jk}(2n_j, 2n_k)}^2$$

$$\times \langle W_i^4 \rangle_{p_{jk}(2n_j, 2n_k)} - \langle W_i^2 \rangle_{p_{jk}(2n_j, 2n_k)}^3 < 0,$$

$$(i, j, k) = (1, 2, 3),\ (2, 3, 1),\ (3, 1, 2). \tag{39}$$

The hybrid NCCa in Eq. (39) represent 1D intensity NCCa for the field $i$ conditioned by simultaneous detection of $n_j$ photons in field $j$ and $n_k$ photons in field $k$.

For the analyzed 3D field, the conditional fields 1 are less nonclassical than the conditional fields 3, as evidenced in the graphs of Fig. 7 showing the NCDs $\tau$ of the NCCa $C^{Wp,1}$ and $M^{Wp,1}$ belonging to conditional fields 1 and $C^{Wp,3}$ and $M^{Wp,3}$ quantifying the nonclassicality of conditional fields 3. The NCCa $C^{Wp,1}$ and $M^{Wp,1}$ ($C^{Wp,3}$ and $M^{Wp,3}$) assign the values of NCDs $\tau$ around 0.2 (0.3) for the conditional fields 1 (3). This asymmetry originates in the structure of the analyzed 3D field. Whereas the nonclassicality in conditional fields 1 is caused by photon pairs residing in the fields 13 and 23 whose numbers are chosen by "two-step" postselection based on the detection of given numbers of photons in the fields 2 and 3, the nonclassicality of conditional fields 3 has its origin in both types of photon pairs (residing in fields 13 and 23) and independent postselections requiring the detection of given numbers of photons in the fields 1 and 2.

## VIII. CONCLUSIONS

Using the Cauchy-Schwarz inequality, non-negative quadratic forms, the majorization theory and non-negative polynomials we have formulated large groups of nonclassicality criteria for general $N$-dimensional optical fields. The nonclassicality criteria were written in intensity moments, probabilities of photon-number distributions and a specific

hybrid form that simultaneously includes both intensity moments and probabilities. The derived nonclassicality criteria were decomposed into the simplest building blocks and then mutually compared. The fundamental nonclassicality criteria suitable for application were identified. As a special example, an *N*-dimensional form of the Hillery nonclassicality criteria was derived.

Discussing the transformation of intensity moments and photon-number distributions between different field-operator orderings, quantification of the nonclassicality based on these criteria and using the nonclassicality depth was accomplished.

The properties as well as the performance of the derived nonclassicality criteria were demonstrated considering an experimental three-dimensional optical field containing two types of photon pairs. It was shown that the intensity nonclassicality criteria are both efficient in revealing the nonclassicality and robust with respect to experimental errors.

The ability of the probability nonclassicality criteria to provide insight into the distribution of nonclassicality across the profile of photon-number distribution was demonstrated. The hybrid nonclassicality criteria were presented as a useful alternative to the intensity and probability nonclassicality criteria.

The analyzed experimental example proved that the nonclassicality criteria represent a very powerful tool in identifying and quantifying the nonclassicality in its various forms. The derived nonclassicality criteria are versatile and as such they can be successfully applied to any optical field.

[1] L. Mandel and E. Wolf, *Optical Coherence and Quantum Optics* (Cambridge University, Cambridge, 1995).

[2] A. Lukš, V. Peřinová, and J. Peřina, Principal squeezing of vacuum fluctuations, Opt. Commun. **67**, 149 (1988).

[3] V. V. Dodonov, Nonclassical states in quantum optics: A squeezed review of the first 75 years, J. Opt. B: Quantum Semiclassical Opt. **4**, R1 (2002).

[4] A. I. Lvovsky and M. G. Raymer, Continuous-variable optical quantum state tomography, Rev. Mod. Phys. **81**, 299 (2009).

[5] J. Peřina, *Quantum Statistics of Linear and Nonlinear Optical Phenomena* (Kluwer, Dordrecht, 1991).

[6] J. Peřina Jr., O. Haderka, and V. Michálek, Non-classicality and entanglement criteria for bipartite optical fields characterized by quadratic detectors II: Criteria based on probabilities, Phys. Rev. A **102**, 043713 (2020).

[7] R. Short and L. Mandel, Observation of Sub-Poissonian Photon Statistics, Phys. Rev. Lett. **51**, 384 (1983).

[8] M. C. Teich and B. E. A. Saleh, Observation of sub-Poisson Franck-Hertz light at 253.7 nm, J. Opt. Soc. Am. B **2**, 275 (1985).

[9] C. T. Lee, Higher-order criteria for nonclassical effects in photon statistics, Phys. Rev. A **41**, 1721 (1990).

[10] A. Allevi, S. Olivares, and M. Bondani, High-order photon-number correlations: A resource for characterization and applications of quantum states, Int. J. Quantum Inform. **10**, 1241003 (2012).

[11] A. Allevi, M. Lamperti, M. Bondani, J. Peřina Jr., V. Michálek, O. Haderka, and R. Machulka, Characterizing the nonclassicality of mesoscopic optical twin-beam states, Phys. Rev. A **88**, 063807 (2013).

[12] J. Sperling, M. Bohmann, W. Vogel, G. Harder, B. Brecht, V. Ansari, and C. Silberhorn, Uncovering Quantum Correlations with Time-Multiplexed Click Detection, Phys. Rev. Lett. **115**, 023601 (2015).

[13] G. Harder, T. J. Bartley, A. E. Lita, S. W. Nam, T. Gerrits, and C. Silberhorn, Single-Mode Parametric-Down-Conversion States with 50 Photons as a Source for Mesoscopic Quantum Optics, Phys. Rev. Lett. **116**, 143601 (2016).

[14] O. S. Magańa-Loaiza, R. de J. León-Montiel, A. Perez-Leija, A. B. U'Ren, C. You, K. Busch, A. E. Lita, S. W. Nam, R. P. Mirin, and T. Gerrits, Multiphoton quantum-state engineering using conditional measurements, npj Quantum Inf. **5**, 80 (2019).

[15] J. Peřina Jr., V. Michálek, R. Machulka, and O. Haderka, Two-beam light with simultaneous anti-correlations in photon-number fluctuations and sub-Poissonian statistics, Phys. Rev. A **104**, 013712 (2021).

[16] J. Peřina Jr., V. Michálek, R. Machulka, and O. Haderka, Two-beam light with 'checkered-pattern' photon-number distributions, Opt. Express **29**, 29704 (2021).

[17] I. I. Arkhipov, J. Peřina Jr., V. Michálek, and O. Haderka, Experimental detection of nonclassicality of single-mode fields via intensity moments, Opt. Express **24**, 29496 (2016).

[18] J. Peřina Jr., I. I. Arkhipov, V. Michálek, and O. Haderka, Nonclassicality and entanglement criteria for bipartite optical fields characterized by quadratic detectors, Phys. Rev. A **96**, 043845 (2017).

[19] D. N. Klyshko, Observable signs of nonclassical light, Phys. Lett. A **213**, 7 (1996).

[20] E. Waks, E. Diamanti, B. C. Sanders, S. D. Bartlett, and Y. Yamamoto, Direct Observation of Nonclassical Photon Statistics in Parametric Down-Conversion, Phys. Rev. Lett. **92**, 113602 (2004).

[21] E. Waks, B. C. Sanders, E. Diamanti, and Y. Yamamoto, Highly nonclassical photon statistics in parametric down-conversion, Phys. Rev. A **73**, 033814 (2006).

[22] K. Wakui, Y. Eto, H. Benichi, S. Izumi, T. Yanagida, K. Ema, T. Numata, D. Fukuda, M. Takeoka, and M. Sasaki, Ultrabroadband direct detection of nonclassical photon statistics at telecom wavelength, Sci. Rep. **4**, 4535 (2014).

[23] J. Peřina Jr., V. Michálek, and O. Haderka, Higher-order sub-Poissonian-like nonclassical fields: Theoretical and experimental comparison, Phys. Rev. A **96**, 033852 (2017).

[24] J. Peřina Jr., V. Michálek, and O. Haderka, Non-classicality of optical fields as observed in photocount and photon-number distributions, Opt. Express **28**, 32620 (2020).

[25] M. V. Chekhova, O. A. Ivanova, V. Berardi, and A. Garuccio, Spectral properties of three-photon entangled states generated

via three-photon parametric down-conversion in a $\chi^{(3)}$ medium, Phys. Rev. A **72**, 023818 (2005).

[26] L. K. Shalm, D. R. Hamel, Z. Yan, C. Simon, K. J. Resch, and T. Jennewein, Three-photon energy-time entanglement, Nat. Phys. **9**, 19 (2013).

[27] D. R. Hamel, L. K. Shalm, H. Hubel, A. J. Miller, F. Marsili, V. B. Verma, R. P. Mirin, S. W. Nam, K. J. Resch, and T. Jennewein, Direct generation of three-photon polarization entanglement, Nat. Photonics **8**, 801 (2014).

[28] B. Alexander, J. J. Bollinger, and H. Uys, Generating Greenberger-Horne-Zeilinger states with squeezing and postselection, Phys. Rev. A **101**, 062303 (2020).

[29] M. Hillery, Conservation laws and nonclassical states in nonlinear optical systems, Phys. Rev. A **31**, 338 (1985).

[30] C. T. Lee, Measure of the nonclassicality of nonclassical states, Phys. Rev. A **44**, R2775 (1991).

[31] J. Peřina Jr., O. Haderka, and V. Michálek, Simultaneous observation of higher-order non-classicalities based on experimental photocount moments and probabilities, Sci. Rep. **9**, 8961 (2019).

[32] B. Kuhn, W. Vogel, and J. Sperling, Displaced photon-number entanglement tests, Phys. Rev. A **96**, 032306 (2017).

[33] I. I. Arkhipov, Complete identification of nonclassicality of Gaussian states via intensity moments, Phys. Rev. A **98**, 021803(R) (2018).

[34] G. S. Agarwal and K. Tara, Nonclassical character of states exhibiting no squeezing or sub-Poissonian statistics, Phys. Rev. A **46**, 485 (1992).

[35] E. Shchukin, T. Richter, and W. Vogel, Nonclassicality criteria in terms of moments, Phys. Rev. A **71**, 011802(R) (2005).

[36] W. Vogel, Nonclassical Correlation Properties of Radiation Fields, Phys. Rev. Lett. **100**, 013605 (2008).

[37] A. Miranowicz, M. Bartkowiak, X. Wang, Y.-X. Liu, and F. Nori, Testing nonclassicality in multimode fields: A unified derivation of classical inequalities, Phys. Rev. A **82**, 013824 (2010).

[38] A. W. Marshall, I. Olkin, and B. C. Arnold, *Inequalities: Theory of Majorization and its Application,* 2nd ed. (Springer, New York, 2010).

[39] C. T. Lee, General criteria for nonclassical photon statistics in multimode radiations, Opt. Lett. **15**, 1386 (1990).

[40] A. P. Dempster, N. M. Laird, and D. B. Rubin, Maximum likelihood from incomplete data via the EM algorithm, J. Royal Statist. Soc. B **39**, 1 (1977).

[41] Y. Vardi and D. Lee, From image deblurring to optimal investments: Maximum likelihood solutions for positive linear inverse problems, J. Royal Statist. Soc. B **55**, 569 (1993).

[42] P. M. Morse and H. Feshbach, *Methods of Theoretical Physics* (McGraw-Hill, Amsterdam, 1953), Vol. 1.